ACS APPLIED MATERIALS & INTERFACES

Letter

www.acsami.org

Effective Indium-Doped Zinc Oxide Buffer Layer on Silver Nanowires for Electrically Highly Stable, Flexible, Transparent, and Conductive Composite Electrodes

Hyun Jun Lee,[†] Ju Hyun Hwang,[†] Kyung Bok Choi,[†] Sun-Gyu Jung,[†] Kyu Nyun Kim,[†] Yong Sub Shim,[†] Cheol Hwee Park,[†] Young Wook Park,[‡,*] and Byeong-Kwon Ju[†,*]

[†]Display and Nanosystem Laboratory, College of Engineering, Korea University, Seoul 136-713, Republic of Korea

[‡]The Institute of High Technology Materials and Devices, Korea University, Seoul 136-713, Republic of Korea

ABSTRACT: We demonstrate a flexible, transparent, and conductive composite electrode comprising silver nanowires (Ag NWs), and indium-doped zinc oxide (IZO) layers. IZO is sputtered onto an Ag NW layer, with the unique structural features of the resulting composite suitable as a flexible, transparent, conductive electrode. The IZO buffer layer prohibits surface oxidation of the Ag NW, and is thereby effective in preventing undesirable changes in electrical properties. The newly designed composite electrode is a promising alternative to conventional ITO films for the production of flexible and transparent electrodes to be applied in next-generation flexible electronic devices.

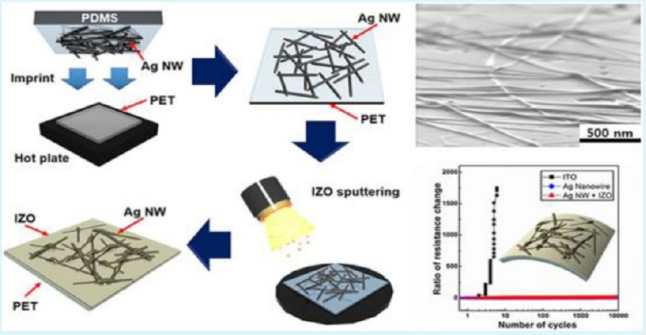

KEYWORDS: *silver nanowire, composite electrode, flexible transparent electrode, oxidation, buffer layer, low-temperature processing*

1. INTRODUCTION

Transparent electrodes have attracted much attention for being critical components of electronic devices, such as touch screen panels, organic light-emitting diodes (OLEDs), and organic solar cells,[1,2] and are essential for optical devices. For next-generation displays, flexibility is required of transparent electrodes, given the renewed interest in innovative flexible devices in recent years.[3]

Currently, the most widely used material for flat-panel display devices is indium tin oxide (ITO), a challenging material to work with in the production of touch panels and a number of other electrical applications.[4] Typically, ITO is sputtered on substrates by physical vapor deposition, with the resultant films known to have a high transmittance (over 90%), and a low sheet resistance (under 30 Ω/sq) at deposition temperatures of 200−350 °C. These properties fully satisfy the required characteristics typical of transparent electrodes, but unfortunately a decrease in transparency, electrical conductivity, and chemical stability has been reported at low deposition temperatures below 150 °C.[5] Since most flexible substrates need a low-temperature for processing, ITO has usually been coated directly onto glass, and not on top of the flexible substrate. Furthermore, ITO is a ceramic material and therefore very brittle and susceptible to cracks.[6] Because of these limiting factors ITO cannot be used in the next generation of flexible displays, and so it is necessary to consider alternative electrode materials to achieve stable performance, and reduced production cost, for industrial production of flexible devices. Therefore, we have focused on the creation of a composite electrode from a new material that is easy to handle, can achieve great conductivities, and is also mechanically flexible.

Among the various promising candidates available for an alternative flexible electrode, many are considered too unstable or too difficult to handle or fabricate, which includes carbon nanotubes,[7] graphene[8] and various polymers.[9] Consequently, commercialization of alternative flexible electrodes has been somewhat delayed, although among the various possible candidates silver Nanowires (Ag NWs) seem to be particularly well suited. Ag NWs have recently attracted a lot of attention because of their transparency, high conductivity, solution processability, and mechanical flexibility when employed as a transparent conductive electrode.[10,11] In addition, the fabrication of Ag NWs can be controlled by using a solution-based process, allowing many techniques such as spraying,[12] dipping,[13] roll-to-roll,[14] and printing for a rapid and simple low-cost production process.[15] Unfortunately, there are a number of serious fundamental issues including oxidation of silver, surface roughness, and a weak mechanical adhesion force, that need to be resolved prior to the adaptation of conventional Ag NW networks.[16,17] Recently, a considerable number of studies have been made on Ag NW electrodes to try and produce high-performance ITO-free devices;[18] however, the research is still lacking when it comes to high-quality Ag NW electrodes for optoelectronic devices.

The key issues with high-quality Ag NW electrodes are the maintenance of the electrical properties under hard chemical

Received: July 1, 2013
Accepted: October 3, 2013
Published: October 3, 2013

and mechanical conditions, and the achievement of a smoother surface morphology. For these reasons, numerous attempts have been made by researchers to improve the properties of Ag NW-based electrodes, including investigations into a large number of different types of chemical treatments and new electrode design types. Pristine Ag NWs require chemical treatments with acetone vapor or hydrogen chloride[19,20] in order to achieve electrochemical stability, and it is well-known that these substances are extremely dangerous, as well as representing serious pollutants to the environment. An alternative method is to combine Ag NWs with another material, such as graphene oxide nanosheets, to produce a composite and thereby resolve some of the intrinsic problems of pure Ag NW networks. Moon et al. demonstrated that graphene oxide nanosheets could be coated onto Ag NW films by a simple spray process;[21] however, single sheets of graphene are hard to produce, and even harder to deposit uniformly onto an appropriate substrate.[22] Therefore, we investigated a newly designed composite Ag NW electrode without dangerous chemical treatments, and with a simple production process, by using an IZO buffer layer. IZO has a stable amorphous structure, with a smooth surface and a high transmittance, and can be deposited at room temperature. The only drawback being that IZO has a relatively low electrical conductivity compared to ITO.[23] Ag NWs of high conductivity solved the problem of the relatively poorly conducting IZO layer, and in this respect, the two materials are complementary to each other. In recent years, therefore, there has been a renewed interest in the combination of favorable properties of newly designed composite electrodes.[24,25]

In this study, we fabricated newly designed semipermanent and flexible composite Ag NW/IZO electrodes, using contact-printed Ag NW films and sputtered IZO layers at low temperature. The electrodes were subsequently investigated with respect to their electrical, optical, structural, mechanical, and electrochemical properties. The sputtered IZO layer can prohibit oxidation of the surface and, consequently, such a buffer layer is effective in preventing undesirable changes in the electrical and chemical properties of the Ag NW composite electrodes. Furthermore, the buffered Ag NW electrodes almost never exhibited a change in electrical resistance, even after thousands of bending test cycles with a radius of 5 mm. The hybridization of Ag NW and IZO to form an electrode is a promising alternative to conventional ITO films for the production of semipermanent, flexible, and transparent electrodes, to be applied in next-generation flexible electronic devices.

2. EXPERIMENTAL SECTION

A solution containing dispersed Ag NWs (supplied by Nanopyxis) was prepared by mixing with 97 wt % isopropyl alcohol (IPA), and 2.5 wt % acetone, at a ratio of 97:2.5:0.5 by weight. Ag NWs used had an average diameter of approximately 45 ± 10 nm, and a length of 25 ± 5 μm. To fabricate the mold and appropriate stamps, we preparedpolydimethylsiloxane (PDMS, Sylgard 184, Dow Corning) by mixing the base and the curing agent to a ratio of 10:1 by weight. The PDMS mixture was then poured onto a flat silicon wafer substrate, and cured for 3 h at 70 °C.

To evaluate the electrical, optical, and flexibility characteristics of the composite Ag NW electrodes, thin films were spin-coated on PDMS stamps at 1000, 2000, and 3000 rpm for 40 s, and subsequently annealed on a hot plate at 80 °C for 3 min. The Ag NW dispersion solution was deposited on a plasma-treated PDMS stamp, preannealed on a hot plate at 80 °C for 3 min, then contact printed onto the top of the substrate. A controlled pressure was applied by using microcontact print equipment at 110 °C for 10 min, to ensure that the contact region at the interface was as conformable as possible. Following this,

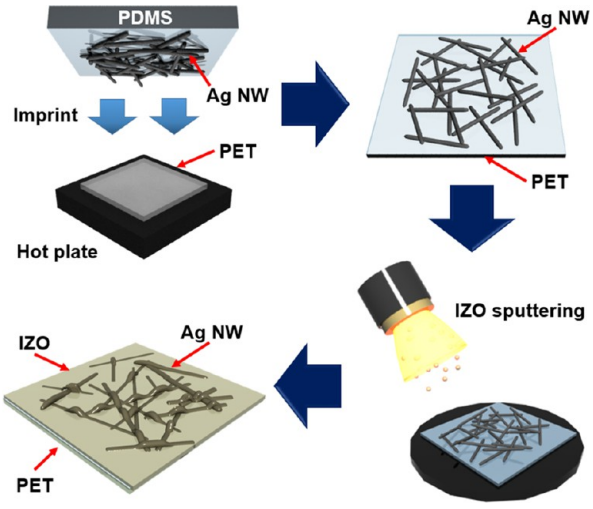

Figure 1. Schematic diagram of the fabrication process of Ag NW/IZO composite electrodes.

a 150 nm thick IZO top layer was sputtered on the transferred Ag NWs using an IZO target at a constant DC power of 150 W, an Ar flow of 4 sccm, and a working pressure of 0.5 mTorr. Figure 1. illustrates the procedure for creating the Ag NW/IZO composite electrodes. Glass substrates were precleaned by ultrasonication in acetone, methanol, and deionized water for 5 min in each solvent, then treated with oxygen plasma under 50 sccm of oxygen at a power of 100 W for 50 s (Cute-MP, Femto Science). In addition, polyethylene terephthalate (PET) substrates were precleaned by the same process sequence, but without acetone treatment. We made the composite electrode on top of the glass substrate just for the EDX, SEM, AFM analysis. But the key is, flexible substrate (PET) was used to electrical properties analysis of composite electrode.

X-ray diffraction (XRD) patterns were recorded using Cu−Kα radiation on a commercial diffractometer (Model D, Rigaku), samples being prepared by placing the film on a glass slide. Surface morphology images of the samples were obtained using field-emission scanning electron microscopy (FE-SEM, S-4800, Hitachi), with elemental mappings conducted by energy-dispersive X-ray spectroscopy (EDX) attached to the S-4800 FE-SEM. Sheet resistances of the films were measured using a four-point probe, with a source measurement unit (FPP-40k, Dasol Eng). The sheet resistance for each sample was measured 10 times, and then averaged.

The optical transmittance characteristics were measured using a UV−vis spectrophotometer (Cary 5000, Varian) in the wavelength range of 300 to 800 nm. The surface morphologies of IZO, pristine Ag NW, and Ag NW/IZO films were measured by atomic force microscopy (AFM, XE-100, Park Systems) in noncontact mode. Cyclic bending tests of the ITO, pristine Ag NW, and Ag NWs/IZO films were conducted in a conventional bending machine (ZB-100,Z-Tech), with a bending angle of 20° to clarify the mechanical flexibility characteristics of the IZO protected Ag NW films. The samples were measured immediately after preparation at room temperature, without any extra passivation treatment.

To evaluate the electrochemical stability of samples, we regularly checked the electrical properties of the samples by repeating the measurement. The composite electrode almost did not oxidize, and optical properties remained unchanged after 500 h.

3. RESULTS AND DISCUSSION

The crystalline nature of the prepared Ag NWs was examined by XRD analysis, with Figure 2. showing the corresponding XRD pattern. The XRD plot shows crystalline diffraction peaks at scattering angles of 2θ = 38.04, 44.76, 64.16, and 77.44°, which can be attributed to the (1 1 1), (2 0 0), (2 2 0), and

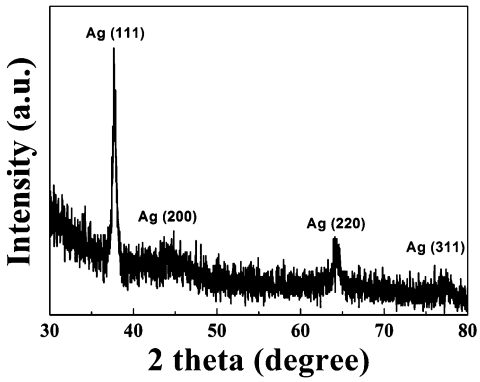

Figure 2. XRD pattern of as-prepared Ag NWs.

(3 1 1) reflections, respectively. All intense XRD peaks can be indexed according to the face-centered-cubic phase of silver.[26]

As mentioned above, because of the nature of Ag, the surface of Ag NWs is easily oxidized in air. It is therefore essential to understand first the mechanism leading to electrochemical change because of oxidation, in order to develop an effectively buffered Ag NW composite electrode. Consequently, to more accurately observe the Ag NW oxidation process, we recorded the chemical composition of coated pristine Ag NWs and Ag NW films as a function of time using SEM and EDX. Images a and b in Figure 3 show two completely different SEM images, the original Ag NWs and the oxidized Ag NW surface after exposure to air for a time of 200 h, respectively. Other research groups have reported a correlation between the electrical properties and oxidation of AgNW,[27] producing SEM images of oxidized Ag NW concordant with our result. The reliability of our results is further supported by the results of experimental analysis by the Murray group.[28] To determine quantitatively the chemical composition of just transferred Ag NWs, and oxidized Ag NWs (200 h after coating), an EDX analysis was performed as shown in panels c and d in Figure 3 . The EDX spectrum definitively proved a composition of silver and oxygen atoms,[29] with the "Ag" peaks originating from the Ag NWs, and the "O" peak from the oxidized NWs surfaces. On the basis of these EDX results, a surface protective layer or other appropriate encapsulation of Ag NW electrodes is certainly required to avoid surface oxidation.

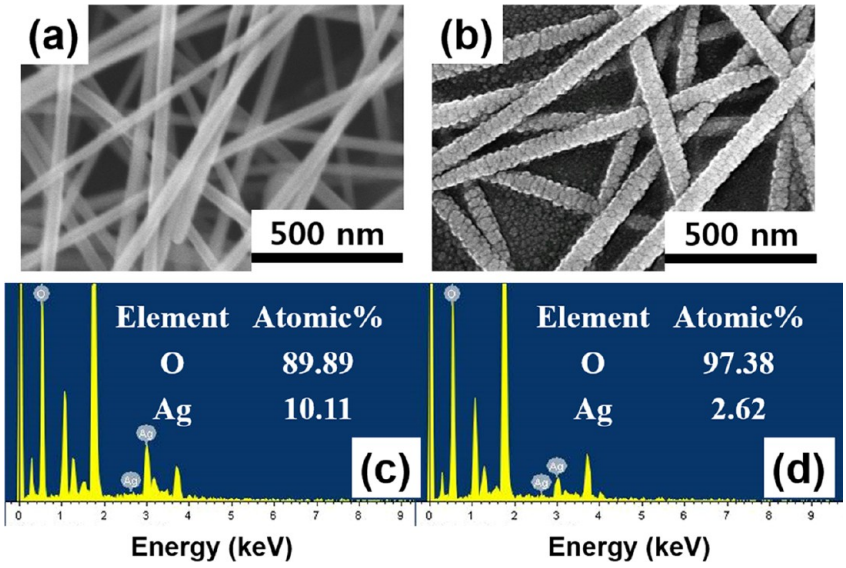

Figure 3. High-resolution SEM images of (a) just transferred Ag NWs and (b) Ag NWs 200 h after coating. (c, d) EDX spectrum showing the quantitative elemental composition of just coated Ag NWs and Ag NWs exposed to air for 200 h.

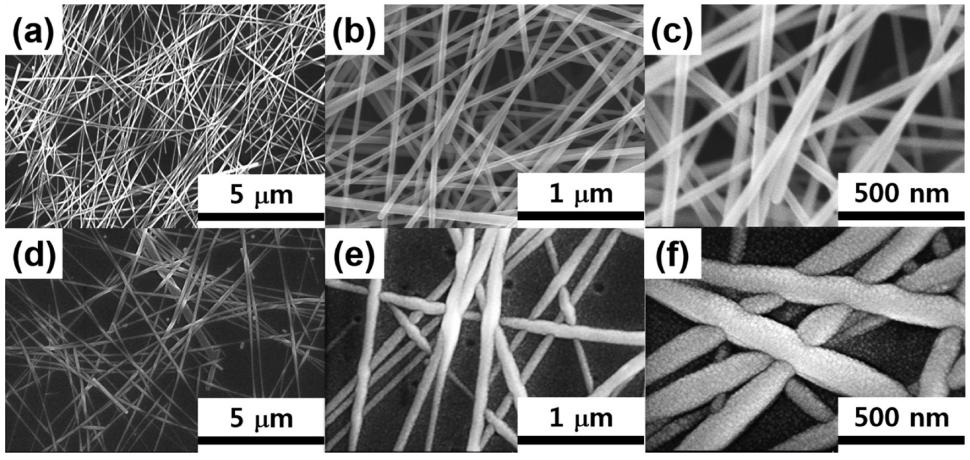

Figure 4. Top view of (a–c) Ag NW random networks and (d–f) strongly welded together composited Ag NW networks.

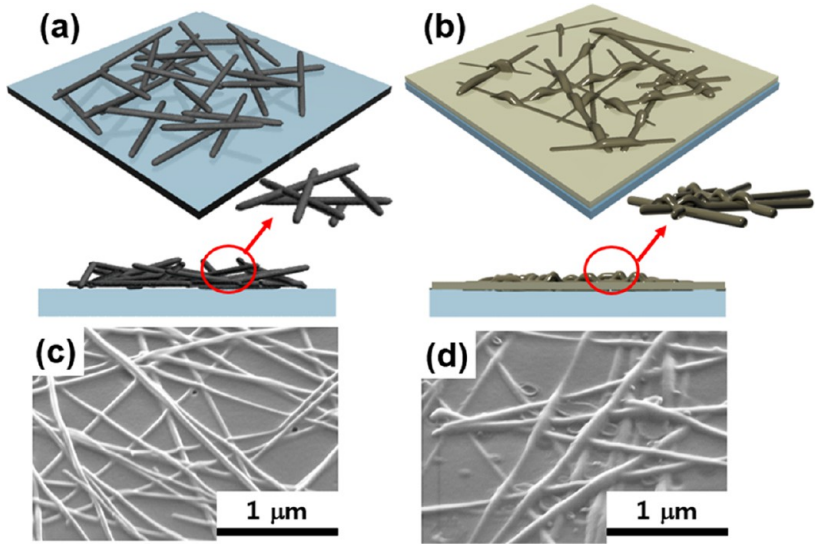

Figure 5. (a, b) Schematic diagram showing the function of just transferred Ag NWs and the IZO buffer layer in reducing the surface roughness and the weld junctions of NWs. (c, d) Tilted cross-sectional SEM image of transferred Ag NWs, a composite Ag NW/IZO film.

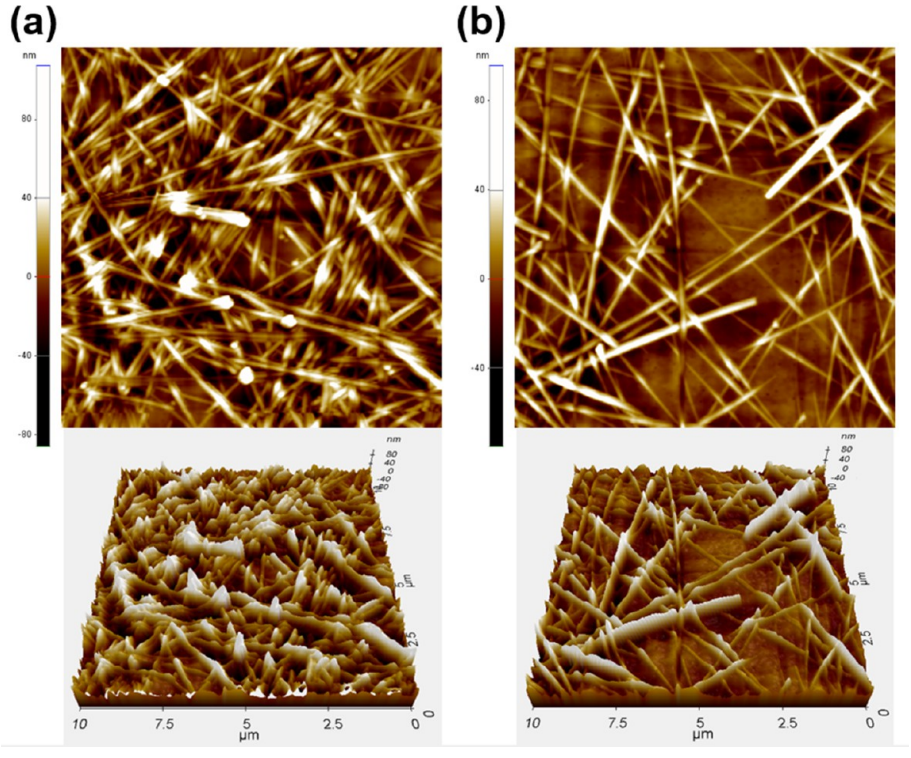

Figure 6. AFM topographic images of (a) pristine Ag NW and (b) a composite Ag NW/IZO film (1 μm × 1 μm), three-dimensional AFM image (down side).

As mentioned above, composite Ag NW/IZO electrodes were fabricated by sputtering an IZO layer on Ag NWs, with SEM imaging performed both before and after deposition of the IZO buffer layer. Before IZO sputtering the entire network consists of individual and distinct thin NWs (Figure 4a–c), whereas after being coated with an IZO layer, the NWs are thicker and welded together (Figure 4d–f).

Panels a and b in Figure 5 show a schematic illustration of Ag NW and fabricated IZO-buffered Ag NW electrode, with the welded NWs resulting in a considerably changed morphology. To determine the mechanism of the conductivity enhancement (19.84 to 11.02 Ω/sq) in the composite Ag NW films, we observed the surfaces of the nanostructures in more detail by SEM. The tilted cross-sectional images of welded Ag NW and Ag NW/IZO electrodes are shown in panels c and d in Figure 5. Prior to the buffering process, the nanowires appear stacked in all directions, without forming junctions; however, this was changed considerably by the presence of the IZO buffer layer, which resulted in junctions being welded together. These network structure changes, and the junction geometry, both in turn create changes in the Ag NW film.

Analysis of the composite Ag NW/IZO film surface was performed by AFM in noncontact mode, characterizing the origin of the conductivity enhancement, and change in surface

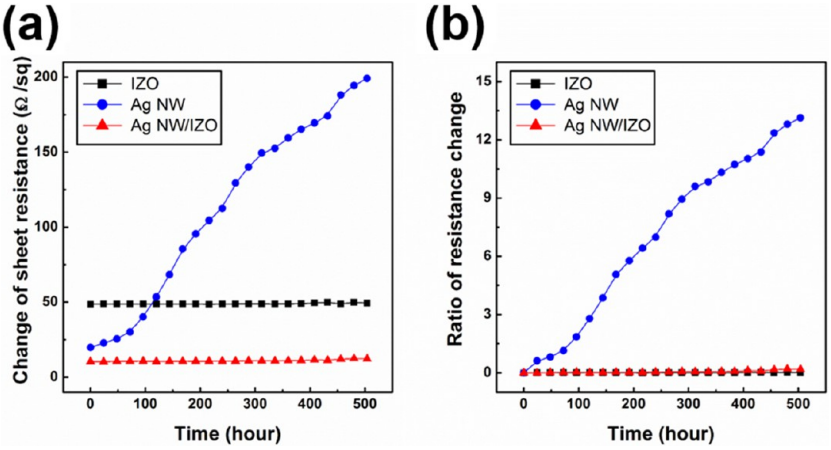

Figure 7. (a) Sheet resistance and (b) ratio of resistance change as a function of exposure time.

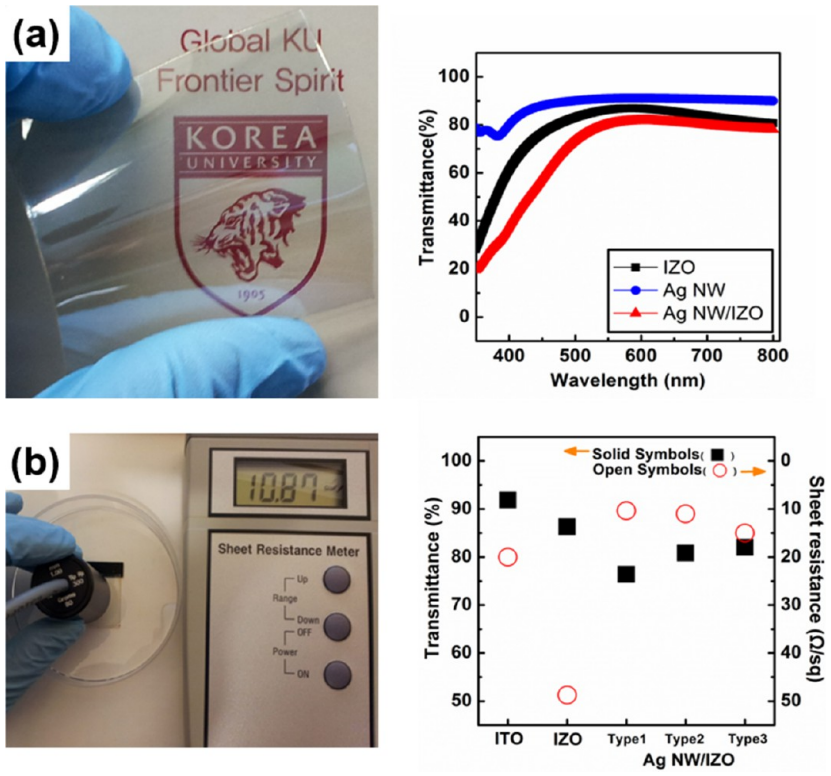

Figure 8. (a) Optical transmittance of IZO and various types of composite Ag NW/IZO films (right side) and image of a composite Ag NW/IZO electrode on a PET film (left side); (b) sheet resistance and optical transmittance at a wavelength of 550 nm of ITO, IZO, and various type of composite Ag NW/IZO films (right side) and image of a sheet resistance measurement of the Ag NW/IZO composite electrode on a PET film (left side).

morphology, by measuring the topographies of a pristine Ag NW film, and a buffered IZO layer on top of a Ag NW film coated on a glass substrate (1 μm × 1 μm). AFM topographic images of the pristine and composite Ag NW films are shown in images a and b in Figure 6, respectively. From these images it is evident that the enclosed IZO particles change the root-mean-square surface roughness (R_q) from more than 21.32 nm, to around 17.03 nm, without any mechanical pressing force. In particular, 3D AFM analysis images were added to show distinctly the unique nanostructure of the film surface, as well as the change in roughness. The surface roughness is a particularly critical factor for Ag NW electrodes used in organic light-emitting diodes (OLED), organic solar cells, and other electronic devices.[30,31]

As mentioned above, the buffering by an IZO layer not only prohibits oxidation of the NWs, but also increases the electrical properties of the composite Ag NW electrode film. Microstructural analysis confirms that the distinctly interconnected shape of the NWs leads to a larger contact area and stronger bonds of the NW network, as compared with pristine Ag NWs, by embedding them into IZO particles. In addition, the contact points were more stable, and the conductive network was more easily formed, with changes in the network structure and firm interconnecting junctions of Ag NWs demonstrably affecting the conductivity. Also evident is a decrease in the sheet resistance, dropping from 19.84 to 11.02 Ω/sq.

dx.doi.org/10.1021/am4025802 | ACS Appl. Mater. Interfaces 2013, 5, 10397−10403

Time-dependent sheet resistance measurements indicate that the sheet resistance of nonbuffered Ag NW films dramatically increases by an order of magnitude after 100 h and, finally, exhibits values approximately 10 times higher after 500 h at room temperature. In comparison, the change in sheet resistance of the IZO film over 500 h is so small as to remain within the margin of error. As expected, the sheet resistance of the IZO buffered Ag NW electrode film was extraordinarily stable over a 500 h period, increasing by only 1.86 Ω/sq, as shown in panels a and b in Figure 7, clearly demonstrating the electrochemical stability of the composite Ag NW electrode film. Figure 8a shows the transmittance of the composite Ag NW electrode with a single pristine Ag NW, ITO, and IZO layer (as reference) at the upper right, and an image of the composite Ag NW/IZO electrode on a PET film (upper left-side). The composite Ag NW layer shows about 80% transmittance in the visible wavelength region. Figure 8b shows the sheet resistance and optical transmittance at a wavelength of 550 nm for ITO, IZO, and various types of composite Ag NW/IZO films (lower right-side frame), as well as an image of a sheet resistance measurement for a composite Ag NW/IZO electrode on a PET film (lower left-side frame). We evaluated various types of Ag NW films with IZO buffer layer, and in order to compare our newly designed composite electrode, we have listed the corresponding figure of merit values for the different coatings of Ag NW in Table 1. The electrode design is optimized for the best figure of merit, which is a parameter commonly used to evaluate transparent conductive electrodes. The electrical sheet resistance (R_s), and the optical transmittance (T) at a wavelength of 550 nm, were used to calculate the figure of merit as defined by Haacke.[32]

$$\Phi_{TC} = T^{10}/R_s$$

This is an objective analysis, but importantly this time we have attempted to extend the range of the rating scale by including an evaluation of the mechanical flexibility, following current research and development activities on flexible electronic devices.

Bending tests were performed to test the flexibility of the composite films, and representative results are indicated in panels a and b in Figure 9. Shown in this figure are the flexibility characteristics of buffered Ag NW flexible films, pristine Ag NW, and ITO. The test was performed with a bending length of 20 mm, and bending radius of 5 mm, with the ratio of the change in resistance of the electrodes recorded as a function of the bending cycle. Resistance changes were recorded 10 times for each bending cycle, in order to ensure sufficient accuracy of the measurement. ITO films are well-known to be fragile and inflexible, and accordingly, the ratio of the resistance changes of the ITO film could not be measured after six bending cycles. In contrast, the composite Ag NW electrode film exhibited an

Table 1. Comparison of the Electrical and Optical Properties of ITO, IZO, Pristine Ag NW, and Composite Ag NW/IZO films

	Characteristics of Various Electrodes		
sample	transmittance (at 550 nm)	sheet resistance (Ω/sq)	figure of merit ($\times 10^{-3}$)
ITO	**0.9185**	**20**	**21.37**
IZO	**0.8629**	**48.73**	**4.70**
Ag NW 1	0.87	19.84	12.52
Ag NW 2	0.9099	24.4	15.94
Ag NW 3	0.9353	30	17.08
Ag NW1/IZO	0.764	10.35	6.55
Ag NW2/IZO	**0.8082**	**11.02**	**12.55**
Ag NW3/IZO	0.8205	15	7.93

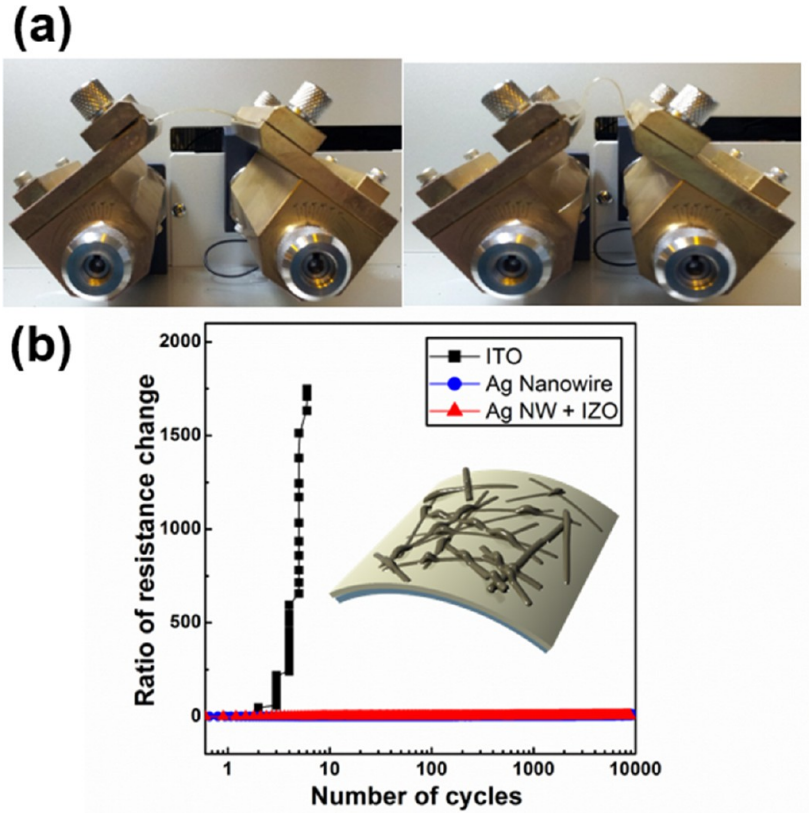

Figure 9. (a) Photograph of the bending tester measuring the mechanical flexibility of the film, (b) ratio of the resistance changes in the bending test.

extraordinarily stable electrical performance, even after more than 10,000 bending tests. Its ability to endure thousands of cycles of mechanical bending is due to the strong adhesion provided by the numerous junction points of the composite electrode film, resulting in a mechanical stability, which in turn will lead to a stable electrical performance of the devices.

In summary, the present results show that by using an IZO buffer layer it is possible to design a new composite Ag NW/IZO film electrode, which exhibits electrochemical stability and enhanced electrical properties and allows for fabrication on a flexible substrate. Consequently, this newly designed film shows promise as a flexible transparent electrode for touch screens, flexible organic solar cells, and flexible OLEDs.

4. CONCLUSION

In conclusion, we have demonstrated the effective use of an IZO buffer layer to achieve highly conductive composite Ag NW films with excellent mechanical properties, stability, and high transparency. In addition, the IZO layer entirely covers the Ag NW, thereby filling empty areas, strongly binding the Ag NW network, and reducing sheet resistance without chemical treatment. More importantly, IZO acts as an encapsulation layer that protects the Ag NW from surface oxidation, thus improving the mechanical and chemical stability of the composite film. Furthermore, the IZO buffered Ag NW film represents a future-oriented electrode, as compared to conventional electrodes using ITO, because its fabrication does not require high temperatures and can be adopted for flexible devices. The newly designed composite electrodes on PET exhibit excellent flexibility, without a significant increase in sheet resistance, even after thousands of bending-test cycles with a curvature radius of 5 mm.

These results lead to the conclusion that the use of an IZO buffer layer for flexible transparent electrodes may enable the development of a broadly applicable, semipermanent, highly conductive electrode in the display industry, and to play an important role in the dissemination of flexible high-performance devices. In conclusion, there is also the possibility of employing this newly designed composite Ag NW/IZO thin film as a promising electrode for semipermanent touch screen panels, and for the flexible optoelectronics industry.

AUTHOR INFORMATION

Corresponding Authors

*E-mail: bkju@korea.ac.kr (B.-K.J.).
*E-mail: zerook@korea.ac.kr(Y.W.P.).

Notes

The authors declare no competing financial interest.

ACKNOWLEDGMENTS

This work was supported by the National Research Foundation of Korea (NRF) under a grant funded by the Korean government (MSIP)(CAFDC/Byeong-Kwon Ju/2007-0056090), the NRF (2012R1A6A3A04039396) Project of the MEST, and the IT R&D Program of MKE/KEIT (2009-F-016-01, Development of Eco-Emotional OLED Flat-Panel Lighting). The authors wish to thank the staff of KBSI for their technical assistance.

REFERENCES

(1) Zeng, X. Y.; Zhang, Q. K.; Yu, R. M.; Lu, C. Z. *Adv. Mater.* **2010**, *22*, 4484−4488.
(2) Lim, J. W.; Cho, D. Y.; Eun, K.; Choa, S. H.; Na, S. I.; Kim, J.; Kim, H. K. *Sol. Energy Mater. Sol. Cells.* **2012**, *105*, 69−76.
(3) Forrest, S. R. *Nature* **2004**, *428*, 911−919.
(4) Kim, H.; Gilmore, C. M.; Piqué, A.; Horwitz, J. S.; Mattoussi, H.; Murata, H.; Kafafi, Z. H.; Chrisey, D. B. *J. Appl. Phys.* **1999**, *86*, 6451−6462.
(5) Hu, Y. L.; Diao, X. G.; Wang, C.; Hao, W. C.; Wang, T. M. *Vacuum.* **2004**, *75*, 183−188.
(6) Chen, Z.; Cotterell, B.; Wang, W. *Eng. Fract. Mech.* **2002**, *69*, 597−603.
(7) Sun, D.-M.; Marina, Y.; Timmermans.; Tian, Y.; Nasibulin, A. G.; Kauppinen, E. I.; Kishimoto, S.; Mizutani, T.; Ohno, Y. *Nat. Nanotechnol.* **2011**, *6*, 156−161.
(8) Han, T.-H.; Lee, Y.; Choi, M.-R.; Woo, S.-H.; Bae, S.-H.; Hong, B. H.; Ahn, J.-H.; Lee, T.-W. *Nat. Photonics* **2012**, *6*, 105−110.
(9) Hwang, J. O.; Park, J. S.; Choi, D, S.; Kim, J. Y.; Lee, S. H.; Lee, K. E.; Kim, Y.-H.; Song, M. H.; Yoo, S.; Kim, S. O. *ACS Nano* **2012**, *6*, 159−167.
(10) Zhu, S.; Gao, Y.; Hu, B.; Li, J.; Su, J.; Fan, Z.; Zhou, Z. *Nanotechnology* **2013**, *24*, 335202.
(11) Sun, Y. *Nanoscale* **2010**, *2*, 1626−1642.
(12) Kim, T.; Canlier, A.; Kim, G. H.; Choi, J.; Park, M.; Han, S. M. *ACS Appl. Mater. Interfaces* **2013**, *5*, 788−794.
(13) Sachse, C.; Müller-Meskamp, L.; Bormann, L.; Kim, Y. H.; Lehnert, F.; Philipp, A.; Beyer, B.; Leo, K. *Org. Electro.* **2012**, *14*, 143−148.
(14) Wu, L. Y. L.; Kerk, W. T.; Wong, C. C. *Thin Solid Films* **2013**, in press.
(15) Kim, T.; Kim, Y. W.; Lee, H. S.; Kim, H.; Yang, W. Y.; Suh, K. S. *Adv. Funct. Mater.* **2013**, *23*, 1250−1255.
(16) Kim, K.; Hong, K.; Koo, B.; Lee, I.; Lee, J.-L. *Appl. Phys. Lett.* **2013**, *102*, 081118.
(17) Wang, Y.; Feng, T.; Wang, K.; Qian, M.; Chen, Y.; Sun, Z. *J. Nanomater.* **2011**, *2011*, 935218.
(18) Groep, J.; Spinelli, P.; Polman, A. *Nano Lett.* **2012**, 3138−3144.
(19) Zhao, B.; Momose, T.; Ohkubo, T.; Shimogaki, Y. *Microelectron. Eng.* **2008**, *85*, 675−681.
(20) Liu, C.-H.; Yu, X. *Nanoscale Res. Lett.* **2011**, *6*, 75.
(21) Moon, I. K.; Kim, J. I.; Lee, H.; Hur, K.; Kim, W. C.; Lee, H. *Sci. Rep.* **2013**, *3*, 1112.
(22) Park, S.; S. Ruoff, R. S. *Nat. Nanotechnol.* **2011**, *4*, 217−224.
(23) Ito, N.; Sato, Y.; Song, P. K.; Kaijio, A.; Inoue, K.; Shigesato, Y. *Thin Solid Films* **2006**, *94*, 99−103.
(24) Kim, Y. S.; Oh, S. B.; Park, J. H.; Cho, M. S.; Lee, Y. *Sol. Energy Mater. Sol. Cells* **2010**, *94*, 471−477.
(25) Ge, J.; Cheng, G.; Chen, L. *Nanoscale* **2011**, *3*, 3084−3088.
(26) Qin, X.; Wang, H.; Miao, Z.; Wang, X.; Fang, Y.; Chen, Q.; Shao, X. *Talanta* **2011**, *84*, 673−678.
(27) Rathmell, A. R.; Nguyen, M.; Chi, M.; Wiley, B. J. *Nano Lett.* **2012**, *12*, 3193−3199.
(28) Murray, B. J.; Newberg, N. T.; Walter, E. C.; Li, Q.; Hemminger, J. C.; Penner, R. M. J. *Anal. Chem.* **2005**, *77*, 5205−5214.
(29) Moore, W. M.; Codella, P. J. *J. Phys. Chem.* **1988**, *92*, 4421−4426.
(30) Coskun, S.; Ates, E. S.; Unalan, H. E. *Nanotechnology* **2013**, *24*, 125202.
(31) Reinhard, M.; Eckstein, R.; Slobodskyy, A.; Lemmer, U.; Colsmann, A. *Org. Electron.* **2012**, *14*, 273−277.
(32) Haacke, G. *J. Appl. Phys.* **1976**, *47*, 4086.